YTUP

Journal of Thermal Engineering

https://jten.yildiz.edu.tr/

https://doi.org/10.47481/jten.0038

RESEARCH ARTICLE

Nonlinear heat transfer analysis of straight fins with temperature-dependent parameters using the finite volume method

Hung Ngoc Huynh[1,*], Vinh-Tan Nguyen[2]

[1]The University of Danang - University of Science and Technology, 54 Nguyen Luong Bang, Danang 550000, Vietnam
[2]Institute of High Performance Computing, Agency for Science Technology and Research (A*STAR), 1 Fusionopolis Way, #16-16 Connexis, 138632, Republic of Singapore

Abstract

This study develops a reliable finite-volume model, implemented in Python, to analyze nonlinear convective–radiative heat transfer in straight fins with nonuniform cross-sections and temperature-dependent properties, which are important in heat exchangers. The one-dimensional steady-state nonlinear equations are solved using Python's fsolve function. Model validation is first performed by comparison with exact solutions in the linear case and, unlike previous studies, is further benchmarked against a three-dimensional solver implemented in the open-source OpenFOAM platform for the nonlinear case, demonstrating excellent agreement in both linear and nonlinear problems. Subsequently, the validated model is applied to investigate the temperature distribution and efficiency of triangular and rectangular fins under varying dimensionless parameters. Results show that ambient fluid temperature affects fin efficiency in contrasting ways depending on whether the thermal conductivity parameter β is positive or negative. Within the investigated ambient temperature range, increasing the dimensionless temperature of the ambient fluid can increase fin efficiency by up to 25% when $\beta < 0$, decrease it by up to 9% when $\beta > 0$, and remain nearly unchanged when $\beta = 0$. Overall, the model provides a valuable framework for investigating nonlinear heat transfer in fins, offering insights into their thermal performance under varying conditions and supporting fin optimization.

Keywords: Fin efficiency, finite volume method, fin simulation, nonlinear heat transfer

Cite this article as: Huynh, H. N., & Nguyen, V. T. (2026). Nonlinear heat transfer analysis of straight fins with temperature-dependent parameters using the finite volume method. Journal of Thermal Engineering, 12(4), 1394–1402. https://doi.org/10.47481/jten.0038

1. Introduction

Extended surfaces, commonly known as fins, are protruding surfaces typically attached to a primary surface to increase surface area and enhance heat dissipation or absorption; they are commonly used in heat exchangers and radiators. A variety of models have been developed and employed to design and analyze the thermal performance of fins. By assuming constant thermal conductivity, assuming a uniform heat transfer coefficient, or neglecting radiation, the models can be simplified to linear problems that are easier to solve analytically. However, many physical phenomena in fins are characterized by nonlinear differential equations. Consequently, approximate analytical and numerical methods are often applied to study nonlinear heat transfer in fins.

A range of approximate analytical techniques has been developed to address nonlinear fin problems, including the Adomian Decomposition Method (ADM) [1–4], the Differential Transformation Method (DTM) [5–10], the Homotopy Analysis Method (HAM) [11, 12], Homotopy Perturbation Method (HPM) [13], and the Variational Iteration Method (VIM) [14]. The advantages of these approximate analytical methods are that they directly solve linear and nonlinear equations without linearization or discretization, and converge rapidly [15, 16]. However, they often require many terms, which makes them less convenient for practical applications [17, 18].

Numerical methods are often employed to verify approximate analytical methods for nonlinear problems. Coşkun et al. [19] used the Finite Element Method (FEM) to benchmark the VIM for a fin with variable heat transfer coefficient, showing strong

*Corresponding Author
E-mail Adress: hnhung@dut.udn.vn

Submitted: 30 July 2025; **Accepted:** 20 November 2025

This paper was recommended for publication in revised form by Editor-in-Chief Ahmet Selim Dalkılıç

Published by Yıldız Technical University, İstanbul, Türkiye
This is an open access article under the CC BY-NC license (http://creativecommons.org/licenses/by-nc/4.0/).

agreement in temperature profiles and fin efficiency. Sobamowo et al [20] employed the Finite Difference Method (FDM) combined with the Crank–Nicolson scheme to validate two approximate models developed for analyzing the transient nonlinear behavior of fins with variable thermal conductivity. The dimensionless temperature distributions obtained from the models were in excellent agreement. Venkitesh and Mallick [21] employed the FDM to validate the HPM in analyzing the heat transfer of porous fins of rectangular and hyperbolic profiles with internal heat generation. The results of temperature distributions showed that the maximum errors occurred at the fin tip. Additionally, Runge–Kutta solutions were used to verify approximate models for nonlinear heat transfer in fins [22, 23].

In parallel with analytical approaches, numerical methods have been widely employed to solve the nonlinear differential equations governing heat transfer in fins. Sobamowo [24] utilized the FDM to analyze a rectangular fin with temperature-dependent thermal conductivity and internal heat generation, validating the solution against the exact linear case. Later, Sobamowo et al. [25] employed the FEM to investigate nonlinear heat transfer in moving porous trapezoidal fins. Although complex nonlinear effects were considered, the results were not validated. In a subsequent work, Sobamowo et al. [26] employed the same numerical approach to study functionally graded rectangular fins under magnetic fields. The results were validated against the exact solution for the linear case. Armin [27] employed the unsteady Galerkin weighted residuals technique to investigate convective-radiative heat transfer through rectangular straight porous fin. Al-Sanea and Mujahid [28] used the Finite Volume Method (FVM) with fully implicit formulation to study the transient case of a rectangular fin with constant properties, findings were benchmarked against analytical results. More recently, Sobamowo et al. [29] applied the FVM to solve nonlinear equations for a convective rectangular longitudinal fin, reporting excellent agreement for the linear case.

Most previous numerical methods, such as FDM, FVM, and FEM, have been validated primarily against analytical solutions for linear cases, thereby limiting confidence in their predictive capability for strongly nonlinear fin problems. In the context of nonlinear heat transfer in extended surfaces, existing numerical methods have primarily focused on rectangular straight fins, leaving other geometries unexplored. Moreover, few studies have leveraged the computational flexibility of modern open-source platforms for nonlinear fin analysis. These gaps highlight the need for an efficient numerical framework, such as the model proposed in this study, to extend reliable nonlinear thermal analysis to a wider range of fin configurations.

The present study develops a numerical model using the FVM to investigate nonlinear heat transfer in longitudinal fins with rectangular and triangular cross-sections. In this model, both thermal conductivity and the heat transfer coefficient vary with temperature. Additionally, a three-dimensional (3D) simulation was conducted using the open-source software OpenFOAM to analyze the fins. The FVM results were validated against analytical solutions for linear cases and 3D model results for nonlinear cases. The model was further used to investigate temperature distributions and fin efficiency.

2. Problem definition

Consider convective and radiative straight fins with uniform and nonuniform cross sections, as shown in Figure 1(a) and (b), respectively. Each fin has a length L, width w and base thickness t_b. The top and bottom surfaces of the fins are exposed to the environment at ambient temperature T_a. For simplicity, the study of fins is based on the following assumptions:

- Steady-state conditions to simplify mathematical formulation.
- The base of each fin is attached to a surface maintained at a constant temperature T_b.
- The fin is investigated in one dimension since the base temperature is uniform across the width of the fin.
- The fin tip, as well as the front and back faces of the fin, is assumed to be adiabatic because heat loss through the tip and thin lateral faces is small compared with heat loss from the main surfaces.

These assumptions are reasonable for thin fins, which are typical in many heat exchangers and electronic cooling applications.

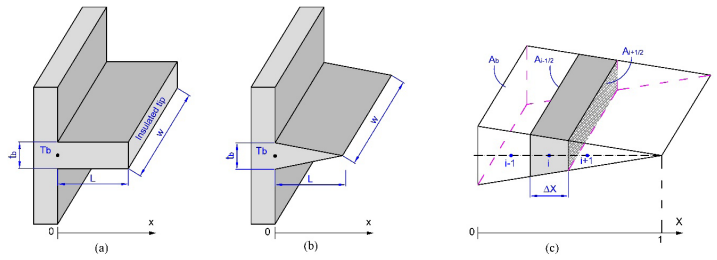

Figure 1. Fin geometries **(a)** straight fin of uniform cross section, **(b)** straight fin of nonuniform cross section, and **(c)** sketch of a control volume for triangular fin.

A steady-state differential equation in one dimension, derived from the heat balance of an infinitesimal element dx is expressed as:

$$\frac{d}{dx}\left(A(x)k(T)\frac{dT}{dx}\right) - \frac{h(T)dA_s}{dx}(T - T_a) - \frac{\epsilon\sigma dA_s}{dx}(T^4 - Ts^4) = 0 \quad (1)$$

where ϵ denotes the surface emissivity, T_s is the radiation sink temperature, A(x) represents the cross-sectional area, and dA_s is the differential surface area of the element. The heat transfer coefficient, h(T), and the thermal conductivity, k(T), of the fins are temperature-dependent, and are defined as:

$$k(T) = k_a[1 + \lambda(T - T_a)] \quad (2)$$

$$h(T) = h_b\left(\frac{T - T_a}{T_b - T_a}\right)^m \tag{3}$$

where, k_a is the thermal conductivity of the fin at the ambient temperature T_a, and the parameter λ characterizes the variation in thermal conductivity. h_b represents the base heat transfer coefficient of the fin with temperature T_b, and m is an exponent that describes different heat transfer mechanisms: laminar film boiling or condensation (m = −1/4), laminar free convection (m = 1/4), turbulent free convection (m = 1/3), and nucleate boiling (m = 2) [30]. By introducing dimensionless parameters as follows:

$$X = \frac{x}{L},\ \theta = \frac{T}{T_b},\ \theta_a = \frac{T_a}{T_b},\ A(X) = \frac{A(x)}{A_b},\ \beta = \lambda T_b,$$
$$M^2 = \frac{h_b dA_s T_b^m L^2}{A_b k_a dx (T_b - T_a)^m},\ N_R = \frac{\epsilon\sigma dA_s L^2 T_b^3}{A_b k_a dx} \tag{4}$$

The dimensionless form of Eq. (1) is expressed as:

$$\frac{d}{dX}\left[A(X)K(\theta)\frac{d\theta}{dX}\right] - M^2(\theta - \theta_a)^{m+1} - N_R(\theta^4 - \theta_s^4) = 0,\ 0 \le X \le 1 \tag{5}$$

Where A(X) epresents the dimensionless cross-sectional area. A(X) =1 for a rectangular profile and A(X)=1-X for the triangular profile. $K(\theta)$ denotes the dimensionless thermal conductivity, defined as:

$$K(\theta) = 1 + \beta(\theta - \theta_a) \tag{6}$$

The dimensionless boundary conditions are as follows:

$$X = 0,\ \theta = 1 \text{ ve } X = 1,\ \frac{d\theta}{dX} = 0 \tag{7}$$

To facilitate the simulation in this study, the specific thermo–geometrical parameters of the fin, adjusted from [31], are applied and listed in Table 1.

Table 1. Thermo–geometrical parameters of the fin

Fin parameters	Values
Fin base temperature, T_b	363.15 K
Ambient fluid temperature, T_a	293.15 K
Radiation sink temperature, T_s	293.15 K
Heat transfer at the fin base, h_b	40 W/(m^2.K)
Reference thermal conductivity, k_a	30 W/(m.K)
Surface emissivity, ϵ	0.8
Thickness of the fin base, t_b	0.008 m
Fin length, L	0.05 m
Fin width, w	0.1 m

3. Numerical method

3.1. Finite volume method

In the FVM framework, the fin length is divided into a finite number n of control volumes (CV). Each presented by a central nodal point. Integration of the governing Eq. (5) over the control volume i (i = 1, ..., n), we obtain the following:

$$\int_{CV_i}\left(\frac{d}{dX}\left[A(X)K(\theta)\frac{d\theta}{dX}\right] - M^2(\theta - \theta_a)^{m+1} - N_R(\theta^4 - \theta_s^4)\right)dV = 0 \tag{8}$$

Rewriting Eq. (8) for each control volume, we have

$$\int_{CV_i} A(X)\frac{d}{dX}\left[K(\theta)\frac{d\theta}{dX}\right]dV + \int_{CV_i} K(\theta)\frac{d\theta}{dX}\frac{dA(X)}{dX}dV - \int_{CV_i} M^2(\theta - \theta_a)^{m+1}dV - \int_{CV_i} N_R(\theta^4 - \theta_s^4)dV = 0 \tag{9}$$

By applying integration by parts for the product of two functions, the first integration term of Eq. (9) is expressed as follows:

$$\int_{CV_i}\left(A(X)\frac{d}{dX}\left[K(\theta)\frac{d\theta}{dX}\right]\right)dV = \left(A(X)K(\theta)\frac{d\theta}{dX}\right)\Big|_{i-1/2}^{i+1/2}\overline{A}_i - \int_{CV_i}\left(K(\theta)\frac{d\theta}{dX}\frac{dA(X)}{dX}\right)dV \tag{10}$$

Where $\bar{A}_i$ represents the average cross-sectional area of the control volume i, as illustrated in Figure 1 (c), and is calculated using $\bar{A}_i = (A_{i-1/2} + A_{i+1/2})/2$, where $A_{i-1/2}$ and $A_{i+1/2}$ are the cross-sectional areas of the left and right faces of the control volume i, respectively.

Substituting Eq. (10) into Eq. (9), we obtain the following:

$$\left(A(X)K(\theta)\frac{d\theta}{dX}\right)\Big|_{i-1/2}^{i+1/2}\overline{A}_i \int_{CV_i} M^2(\theta - \theta_a)^{m+1}dV - \int_{CV_i} N_R(\theta^4 - \theta_s^4)dV = 0 \tag{11}$$

For each interior node i, as shown in Figure. 1(c), applying the central difference to Eq. (11) yields the following:

$$A_{i+1/2}K(\theta)_{i+1/2}\left(\frac{\theta_{i+1} - \theta_i}{\Delta X}\right) + A_{i-1/2}K(\theta)_{i-1/2}\left(\frac{\theta_{i-1} - \theta_i}{\Delta X}\right) - M_i^2(\theta_i - \theta_a)^{m+1}\Delta X - N_{Ri}(\theta_i^4 - \theta_s^4)\Delta X = 0,\ \forall i \in [2, n-1] \tag{12}$$

The thermal conductivity on the two faces of the control volume is calculated as the arithmetic average of the temperatures at the centers of the neighboring control volumes as follows:

$$K(\theta)_{i-1/2} = 1 + \beta[(\theta_{i-1} + \theta_i)/2 - \theta_a] \tag{13}$$

$$K(\theta)_{i+1/2} = 1 + \beta[(\theta_{i+1} + \theta_i)/2 - \theta_a] \tag{14}$$

Applying Eq. (11) for the boundary node 1 having Dirichlet boundary condition, we obtain

$$(1+\beta(\theta_b-\theta_a))A_b\left(\frac{\theta_b-\theta_1}{\Delta X/2}\right)+(1+\beta[(\theta_1+\theta_2)/2-\theta_a])A_{i+1/2}\left(\frac{\theta_2-\theta_1}{\Delta X}\right)$$
$$-M^2(\theta_1-\theta_a)^{m+1}\Delta X-N_{R1}(\theta_1^4-\theta s^4)\Delta X=0 \quad (15)$$

Similarly, applying Eq. (11) for the boundary node n with the adiabatic tip, we obtain

$$(1+\beta[(\theta_{n-1}+\theta_n)/2-\theta_a])A_{n-1/2}\left(\frac{\theta_{n-1}-\theta_n}{\Delta X}\right)$$
$$-M^2(\theta_n-\theta_a)^{m+1}\Delta X-N_{Rn}(\theta n^4-\theta s^4)\Delta X=0 \quad (16)$$

By combining Eqs. (12), (15), and (16), n nonlinear algebraic equations are obtained. In this study, these equations are solved using the Python function fsolve, a wrapper for MINPACK's hybrd and hybrj algorithms, with a convergence criterion of 10^{-7}. Pseudocode for the numerical solution using FVM and fsolve:

1. Define the fin geometry, boundary conditions, and temperature-dependent material properties.
2. Discretize the fin domain into n control volumes using the FVM.
3. Initialize the temperature field at environmental temperature.
4. Formulate the system of nonlinear algebraic equations representing the energy balance in each control volume.
5. Solve the system using Python's fsolve function.
6. Check convergence.
7. Post-process results to obtain temperature distribution and fin efficiency.

3.2. OpenFOAM implementation

To benchmark and compare the FVM model, the open-source code OpenFOAM was used to develop a numerical model for simulating heat transfer in three-dimensional longitudinal fins. Steady heat conduction in longitudinal fins is described by the equation of energy conservation written in terms of temperature as:

$$\nabla\cdot(k\nabla T)=0, \quad (17)$$

Where k represents the fin's thermal conductivity. The above governing equation can generally take into account temperature-dependant thermal conductivity k(T) with the following boundary conditions applied along surfaces of the fins

$$T=T_b,\ x\in\Gamma_b \quad (18)$$

$$-k\frac{dT}{dn}=q_a,\ x\in\Gamma_a \quad (19)$$

Here, the temperature at the base surface Γ_b is set to T_b, while the heat flux q_a is specified for the remaining boundaries exposed to the surrounding environment. The heat flux applied at the exposed surfaces is calculated from the temperature dependent heat transfer coefficient h(T) following Eq. (3) and being zero for surfaces assumed to be adiabatic. All thermal geometrical parameters were obtained from Table 1 to ensure consistency with the one-dimensional FVM approach. The solver was implemented in the OpenFOAM framework to solve the temperature distribution across different fin geometries. For all the simulations using OpenFOAM, the second-order central difference scheme with non-orthogonal correction was used for the discretization of the Laplacian term in Eq. (17). The preconditioned conjugate gradient (PCG) linear solver with diagonal incomplete-Cholesky (DIC) preconditioning is used for solving temperature until convergence criteria of 10^{-7}.

4. Fin efficiency

The fin efficiency is determined as follows:

$$\eta=\frac{\dot{Q}_f}{\dot{Q}_{ideal}}=\frac{\sum_{i=1}^{n}\left(h_b\left(\frac{T_i-T_a}{T_b-T_a}\right)^m dA_{si}(T_i-T_a)+\epsilon\sigma dA_{si}(Ti^4-Ts^4)\right)}{\sum_{i=1}^{n}(h_b dA_{si}(T_b-T_a)+\epsilon\sigma dA_{si}(Tb^4-Ts^4))} \quad (20)$$

Where $\dot{Q}_f$ and $\dot{Q}_{ideal}$ represent the actual and ideal heat transfer, respectively. Also, the fin efficiency can be calculated based on the dimensionless parameters as follows:

$$\eta=\frac{\sum_{i=1}^{n}(M_i^2(\theta_i-\theta_a)^{m+1}+N_{Ri}(\theta_i^4-\theta_s^4))}{\sum_{i=1}^{n}(M_i^2(1-\theta_a)^{m+1}+N_{Ri}(1-\theta_s^4))} \quad (21)$$

5. Results and discussion

Due to the lack of an exact solution for the nonlinear case, the two models were first validated against the exact solution for the linear case. From Eq. (5), the validated linear case corresponds to a rectangular fin with exponential constant m = 0, thermal conductivity parameter $\beta = 0$, and surface emissivity $\epsilon = 0$. According to [32], the analytical solutions for the temperature (θ_{exact}) and heat transfer ($\dot{Q}_{exact}$) of a linear rectangular fin are given as follows:

$$\theta_{exact}=\theta_a+(1-\theta_a)\frac{\cosh(m_0(L-x))}{\cosh(m_0L)} \quad (22)$$

$$\dot{Q}_{f,exact}=\sqrt{h_b P k_a A}(T_b-T_a)\tanh(m_0L) \quad (23)$$

Where $m_0=\sqrt{h_b P/(k_a A)}$ and P are the fin perimeter.

For the nonlinear case, the FVM results were compared with OpenFOAM results with the exponential constant m = 1/3 (this represents turbulent natural convection), the thermal conductive parameter $\beta = 0.5$, and the surface emissivity $\epsilon = 0.8$ for both the triangular and rectangular fin profiles. For quantitative assessment, the mean relative error of the dimensionless temperature between the FVM solution and the exact solution for a fin discretized into n control volumes is employed as follows:

$$\epsilon_{error} = \frac{1}{n}\sum_{i=1}^{n} \frac{|\theta_{i,FVM} - \theta_{i,exact}|}{\theta_{i,exact}} \times 100 \quad (24)$$

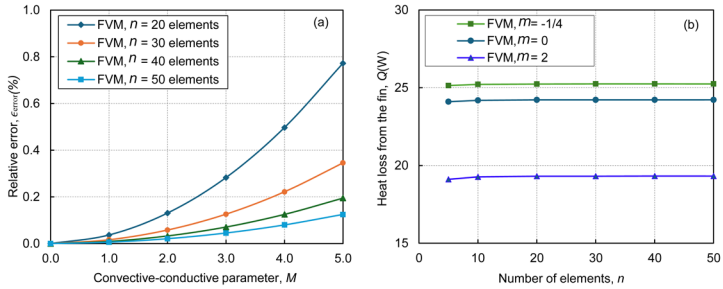

Figure 2. Effect of mesh size on the computed heat transfer rate for fins with a rectangular profile: **(a)** Relative error between the FVM and exact solution for the linear case with m = 0, β = 0, ϵ = 0, and **(b)** dependence of mesh size on heat transfer rate for different values of m in the nonlinear case with β = 0.5, ϵ = 0.8.

Grid independence was verified by employing various grid densities within the range M ∈ [0,5]. The results indicate that the fin efficiency decreases with increasing M and falls below 20% when M ≥ 5. Therefore, investigating values of M greater than 5 is not practical. For the linear case, shown in Figure 2(a), The FVM relative error compared to the analytical solution increases with M and reaches its maximum at M = 5. With a 30-element grid, the maximum error remains below 0.4%, satisfying the convergence criterion. For the nonlinear model (Figure. 2(b),) a comparison between 30- and 40-element grids yields errors of only 0.005% (for m = −1/4) and 0.013% (for m = 2). Hence, a resolution of 30 elements along the fin length was deemed sufficient to ensure grid independence and was adopted throughout this study.

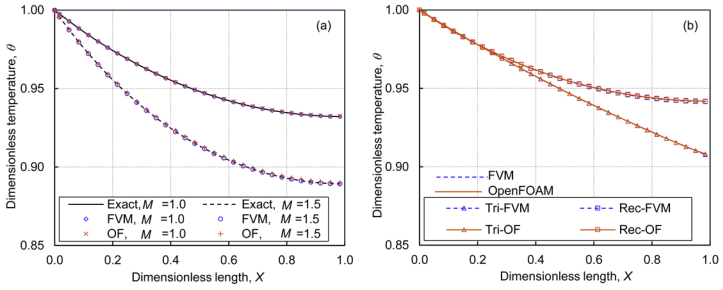

Figure 3. Comparison of the dimensionless temperature distribution θ (X) predicted by the developed FVM model with results from **(a)** OpenFOAM and the exact analytical solution for a rectangular fin (m = 0, β = 0, ϵ = 0), and **(b)** OpenFOAM for triangular and rectangular fins in the nonlinear case (m = 1/3, β = 0.5, ϵ = 0.8).

The validation of the FVM and OpenFOAM model for the linear and nonlinear problems is presented in Figure 3. For the linear case, the FVM results show excellent agreement with the exact solution for both parameters M = 1 and M = 1.5, with the mean relative errors of 0.002% and 0.003%, respectively. Additionally, good agreement was found for the OpenFOAM model, with corresponding errors of 0.021% and 0.061%. In the nonlinear case, a close match was also observed between the FVM and OpenFOAM results, with the mean relative error of the FVM compared to OpenFOAM equal to 0.009% for the triangular profile and 0.02% for the rectangular profile. The temperature contours for both fins, obtained from the OpenFOAM model, are presented in Figure 4, in which the triangular fin exhibits a higher temperature gradient along its length than the rectangular fin. Because the problem size was relatively small, both the present solver and OpenFOAM completed the computation within a few seconds, and no significant difference in CPU time was observed. Therefore, the comparison focuses on accuracy and numerical reliability rather than computational speed.

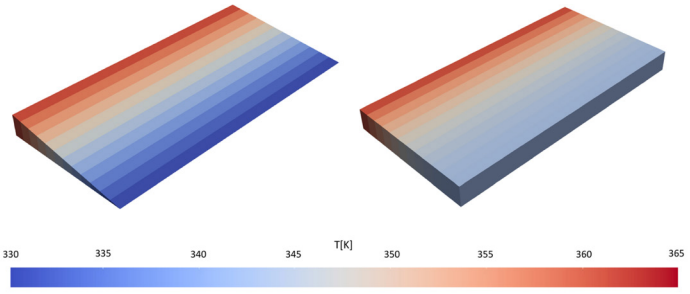

Figure 4. Temperature contour obtained from the OpenFOAM model with m = 1/3, β = 0.5, ϵ = 0.8 of the triangular fin (left) and rectangular fin (right).

Figure 5 presents the impact of the thermal conductivity parameter β on the temperature profiles of both fins, using the FVM and OpenFOAM. There is a strong agreement between the results of the two models. The largest mean relative errors occur for the cases with the thermal conductive parameter β = -1: 0.014% and 0.027% for the triangle and rectangular profiles, respectively. It is observed that an increase in the thermal conductive parameter β leads to higher temperature values within the fins.

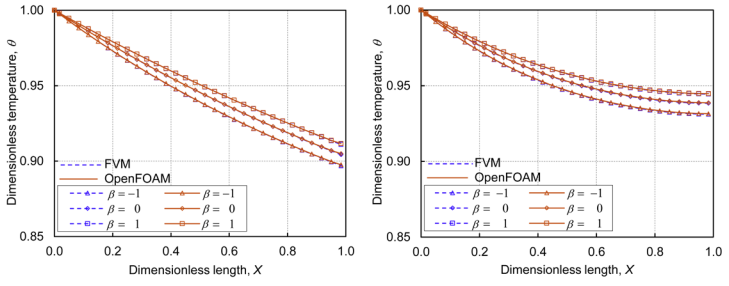

Figure 5. Dimensionless temperature distribution obtained from the FVM and OpenFOAM model with different values of β for the rectangular profile (left), and triangular profile (right).

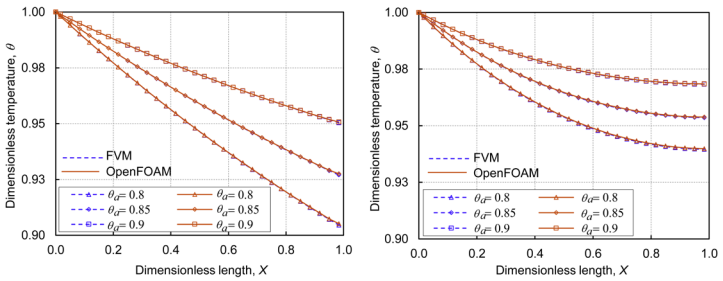

Figure 6. Dimensionless temperature distribution obtained from the FVM and OpenFOAM solutions with different values of θ_a for the rectangular profile (left), and triangular profile (right)

Figure 6 presents the temperature distribution of the two fin profiles under different ambient temperatures using FVM and OpenFOAM. The results demonstrate excellent agreement between the two models, with the highest mean relative error being found for the case with the ambient fluid temperature $\theta_a = 0.8$ being 0.012% and 0.021% for the triangular and rectangular fins, respectively. The fin temperature rises as the ambient fluid temperature increases.

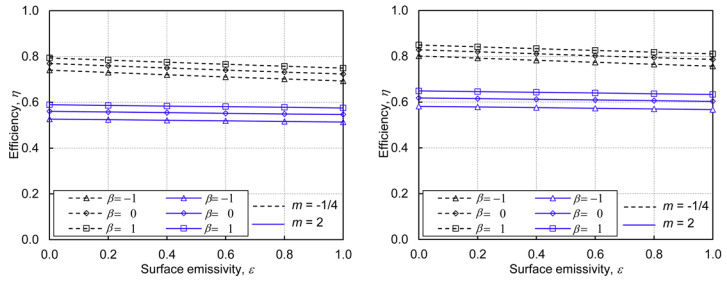

Figure 7. Thermal efficiency obtained from the FVM with different values of m, ϵ and β for the rectangular profile (left), and triangular profile (right)

Figure 7 shows the fin efficiency as a function of β, exponential constant m and surface emissivity ϵ for the two profiles using the FVM. The efficiency of the fins increases when β increases and the significant higher efficiency found for the case with m = -1/4 compared to the case having m =2. Increasing the fin surface emissivity has little impact on efficiency, since radiative heat transfer is minimal due to the small temperature difference with the ambient. Table 2 compares the efficiency of the fins using both the FVM and OpenFOAM solution with various values of β, m and ϵ. The comparison demonstrates strong agreement between the FVM and the OpenFOAM model.

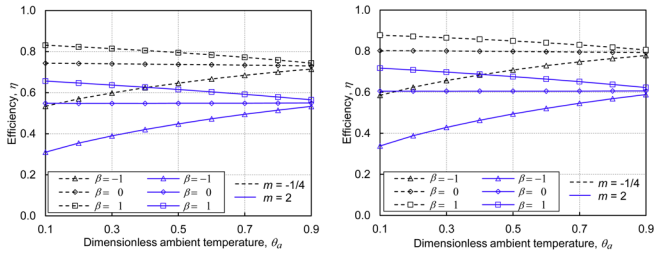

Figure 8. Variation of thermal efficiency predicted by the FVM for different values of m, β and θ_a for the rectangular profile (left), and triangular profile (right)

The effect of parameters β, m and θ_a on the fin efficiency is shown in Figure 8. It is observed that, at the same ambient fluid temperature, the fin efficiency increases with increasing β. This is because, as β increases, the temperature increases, the fin also increases, as shown in Figure 5, consequently, the heat transfer $\dot{Q}_f$, as given in Eq. (20), also increases. From Figure 8, it can be observed that within the investigated ambient temperature range, the effect of ambient fluid temperature on fin efficiency depends on the value of β. When β < 0, increasing the dimensionless ambient temperature enhances fin efficiency by up to 22.34% and 25.02% for triangular and rectangular fins, respectively, in the case of m = 2. The corresponding improvements for m = -1/4 are 18.01% and 19.04%. In contrast, when β > 0, the efficiency decreases by 9.13% and 9.44% for m = 2, and by 8.7% and 7.2% for m = -1/4. For β = 0, the efficiency remains nearly unchanged. To clarify this problem, consider the typical case of a rectangular fin. When β < 0, the heat conduction coefficient of the fin decreases as the temperature rises. This results in a steeper gradient of the temperature distribution along the fin, as shown in Figure 5. An increase in the ambient fluid temperature causes a small percentage decrease in $\dot{Q}_f$, expressed as $\dot{Q}_{fi} - \dot{Q}_{fi+1})/\dot{Q}_{fi}$, compared to that of $\dot{Q}_{ideal}$. Consequently, the fin efficiency increases with rising ambient fluid temperature. Conversely, when β > 0, the percentage decrease in $\dot{Q}_f$ is greater than that of $\dot{Q}_{ideal}$, leading to a reduction in fin efficiency. The detailed effects of ambient fluid temperature on $\dot{Q}_f$ and $\dot{Q}_{ideal}$ are shown in Table 3.

Table 2. Comparison of the efficiency of the fins using both the FVM and OpenFOAM

			Triangular case			Rectangular case		
ϵ	m	β	η_{FVM} (%)	η_{of} (%)	err. (%)	η_{FVM} (%)	η_{of} (%)	err. (%)
0.4	-1/4	-1	72.01	72.05	0.05	78.28	78.37	0.12
0.4	-1/4	1	77.49	77.52	0.03	83.32	83.38	0.07
0.8	2	-1	51.63	51.73	0.19	56.99	57.23	0.42
0.8	2	1	57.78	57.86	0.13	63.65	63.84	0.30

Table 3. The effect of θ_a, β on the efficiency of the triangular fin with m = -1/4 from the FVM results.

	β = -1			β = 1		
θ_a	$\dot{Q}_f$	$\dot{Q}_{ideal}$	η(%)	$\dot{Q}_f$	$\dot{Q}_{ideal}$	η(%)
0.3	65.779	109.857	59.88	89.482	109.857	81.45
0.5	51.918	80.282	64.67	63.838	80.282	79.52
0.7	34.041	49.731	68.45	38.389	49.731	77.19
0.9	12.361	17.294	71.48	12.864	17.294	74.38

6. Conclusion

This study investigated straight fins with temperature-dependent properties using a finite-volume numerical model. The nonlinear governing equations for temperature distribution were solved with Python's fsolve function and validated against both exact solutions and OpenFOAM, showing excellent agreement in linear and nonlinear cases. The model was applied to investigate the temperature distribution and efficiency of rectangular and triangular fins over a range of dimensionless parameters. Results show that ambient fluid temperature affects fin efficiency in contrasting ways depending on the thermal conductivity parameter: within the studied range, increasing the ambient fluid temperature can increase efficiency by up to 25% when $\beta < 0$, decrease it by up to 9% when $\beta > 0$, and remain nearly unchanged when $\beta = 0$. The model provides an effective platform for nonlinear thermal analysis and is currently being explored for fin optimization. Future studies could investigate more complex scenarios, such as transient heat transfer, two-dimensional fin geometries, and fins with internal heat generation. Sensitivity or uncertainty analyses could further quantify the influence of parameters on fin performance, thereby broadening the model's applicability.

Nomenclature

A	fin cross-sectional area, m^2
A_b	area of the fin base, m^2
A_s	surface area of a fin element, m^2
CV	control volume
H(θ)	dimensionless heat transfer coefficient
h_b	heat transfer at the fin base, $W.m^{-2}.K^{-1}$
h(T)	variable heat transfer coefficient, $W.m^{-2}.K^{-1}$
K(θ)	dimensionless thermal conductivity
k_a	thermal conductivity at ambient temperature, $W.m^{-1}.K^{-1}$
K(T)	variable thermal conductivity, $W.m^{-1}.K^{-1}$
L	fin's length, m
M	dimensionless convective-conductive parameter
N_R	dimensionless radiative-conductive parameter
m	Exponent describing different heat transfer mech anisms
n	number of control volumes
P	fin parameter, m
$\dot{Q}_f$	heat transfer, W
$\dot{Q}_{ideal}$	ideal heat transfer, W
T_a	temperature of ambient fluid, K
T_b	temperature at fin base, K
T_s	radiation sink temperature, K
t_b	thickness of the fin base, m
X	dimensionless distance from the fin base
x	distance from the fin base, m
w	fin's width, m

Greek symbols

a	thermal diffusivity, m^2s^{-1}
β	thermal conductivity parameter
ϵ	surface emissivity of the fins
ϵ_{error}	mean relative error
η	fin efficiency
θ	dimensionless temperature
λ	parameter defining the variation of k(T),K^{-1}
ρ	specific density, $kg.m^{-3}$
σ	Stefan–Boltzmann constant, $W.m^{-2}.K^{-4}$

References

[1] Akinshilo A. Analytical decomposition solutions for heat transfer on straight fins with temperature dependent thermal conductivity and internal heat generation. Journal of Thermal Engineering 2019;5:76–92. doi:https://doi.org/10.18186/thermal.505489.

[2] Chiu CH, et al. A decomposition method for solving the convective longitudinal fins with variable thermal conductivity. International Journal of Heat and Mass Transfer 2002;45:2067–2075. doi:10.1016/S0017-9310(01)00286-1.

[3] Arslanturk C. A decomposition method for fin efficiency of convective straight fins with temperature-dependent thermal conductivity. International communications in heat and mass transfer 2005;32:831–841. doi:10.1016/j.icheatmasstransfer.2004.10.006.

[4] Chang MH. A decomposition solution for fins with temperature dependent surface heat flux. International Journal of Heat and Mass Transfer 2005;48:1819–1824. doi:10.1016/j.ijheatmasstransfer.2004.07.049.

[5] Ananth Subray P, Hanumagowda B, Varma S, Zidan A, Kbiri Alaoui M, Raju C, Shah NA, Junsawang P. Dynamics of heat transfer analysis of convective-radiative fins with variable

thermal conductivity and heat generation: Differential transformation method. Mathematics 2022;10:3814. doi:https://doi.org/10.3390/math10203814.

[6] Gireesha B, Sowmya G. Heat transfer analysis of an inclined porous fin using differential transform method. International Journal of Ambient Energy 2022;43:3189–3195. doi:https://doi.org/10.1080/01430750.2020.1818619.

[7] Sadri S, Raveshi MR, Amiri S. Efficiency analysis of straight fin with variable heat transfer coefficient and thermal conductivity. Journal of mechanical science and technology 2012;26:1283–1290. doi:10.1007/s12206-012-0202-4.

[8] Ndlovu PL, Moitsheki RJ. Analytical solutions for steady heat transfer in longitudinal fins with temperature-dependent properties. Mathematical Problems in Engineering 2013;2013:273052. doi:10.1155/2013/273052.

[9] Sobamowo M, Adeleye O, Yinusa A, Oyekeye M, Waheed M. Significance of fin tip temperature on the heat transfer rate and thermal efficiency of a convective-radiative rectangular fin with variable thermal conductivity. Journal of Engineering and Thermal Sciences 2021;1:65–80. doi:https://doi.org/10.21595/jets.2021.22282.

[10] Kundu B. Thermal analysis on variable thickness absorber plate fin in flat-plate solar collectors using differential transform method. Journal of Thermal Engineering 2020;6:157–169. doi:https://doi.org/10.18186/thermal.672169.

[11] Khani F, Aziz A. Thermal analysis of a longitudinal trapezoidal fin with temperature-dependent thermal conductivity and heat transfercoefficient. Communications in Nonlinear Science and Numerical Simulation 2010;15:590–601. doi:10.1016/j.cnsns.2009.04.028.

[12] Domairry G, Fazeli M. Homotopy analysis method to determine the fin efficiency of convective straight fins with temperature-dependent thermal conductivity. Communications in Nonlinear Science and Numerical Simulation 2009;14:489–499. doi:10.1016/j.cnsns. 2007.09.007.

[13] Jalili P, Jalili B, Ahmad I, Hendy AS, Ali MR, Ganji DD. Python approach for using homotopy perturbation method to investigate heat transfer problems. Case Studies in Thermal Engineering 2024;54:104049. doi:https://doi.org/10.1016/j.csite.2024.104049.

[14] Atay M. TS, Cos¸kun B. Comparative analysis of power-law fin-type problems using variational iteration method and finite element method. Mathematical Problems in Engineering 2008;635231. doi:10.1155/2008/635231.

[15] Inc M. Application of homotopy analysis method for fin efficiency of convective straight fins with temperature-dependent thermal conductivity. Mathematics and Computers in Simulation 2008;79:189–200. doi:10.1016/j.matcom.2007.11.009.

[16] Moore TJ, Jones MR. Solving nonlinear heat transfer problems using variation of parameters, International Journal of Thermal Sciences 2015;93:29–35. doi:10.1016/j.ijthermalsci.2015.02.002.

[17] Oguntala G, Abd-Alhameed R, Sobamowo G, Danjuma I. Performance, thermal stability and optimum design analyses of rectangular fin with temperature-dependent thermal properties and internal heat generation. Journal of Computational Applied Mechanics 2018;49:37–43. doi:10.22059/jcamech.2017.244988.203.

[18] Turkyilmazoglu M. Exact solutions to heat transfer in straight fins of varying exponential shape having temperature dependent properties. International Journal of Thermal Sciences 2012;55:69–75. doi:10.1016/j.ijthermalsci.2011.12.019.

[19] Coskun SB, Atay MT. Fin efficiency analysis of convective straight fins with temperature dependent thermal conductivity using variational iteration method. Applied Thermal Engineering 2008;28:2345–2352, https://doi.org/10.1016/j.applthermaleng.2008.01.012.

[20] Sobamowo GM, Dere ZO, Yinusa AA. Nonlinear transient thermal analysis of a convective–radiative fin: A comparative study of two approximate analytical methods. Decision Analytics Journal 2022;5:100133. doi:10.1016/j.dajour.2022.100133.

[21] Venkitesh V, Mallick A. Thermal analysis of a convective–conductive–radiative annular porous fin with variable thermal parameters and internal heat generation. Journal of Thermal Analysis and Calorimetry 2022;147:1519–1533. doi:10.1007/s10973-020-10384-9.

[22] Joneidi A, Ganji D, Babaelahi M. Differential transformation method to determine fin efficiency of convective straight fins with temperature dependent thermal conductivity. International Communications in Heat and Mass Transfer 2009;36:757–762. doi:https://doi.org/10.1016/j.icheatmasstransfer.2009.03.020

[23] Dogonchi A, Ganji D. Convection–radiation heat transfer study of moving fin with temperature-dependent thermal conductivity, heat transfer coefficient and heat generation. Applied thermal engineering 2016;103:705–712. doi:10.1016/j.applthermaleng.2016.04.121.

[24] Sobamowo M. Analysis of convective longitudinal fin with temperature-dependent thermal conductivity and internal heat generation. Alexandria Engineering Journal 2017;56:1–11. doi:10.1016/j.aej.2016.04.022.

[25] Sobamowo M, Salami M, Yinusa A. Thermal analysis of a convective-radiative moving porous trapezoidal fin with variable thermal properties and internal heat generation using finite element method. World Scientific News 2022;163:139–157.

[26] Sobamowo GM, Yinusa AA, Salami MO, Abubakar HE. Finite element analysis of transient thermal behaviour of a radiative-convective fin with functionally graded material under the influence of magnetic field: Finite element analysis of transient thermal behaviour of a radiative-convective fin. Journal of Complex Flow 2023;5:31–38.

[27] Emamıfar A, Moghadası H, Noroozı MJ, Saffarı H. Transient analysis of convective-radiative heat transfer through porous fins with temperature-dependent thermal conduc-

tivity and internal heat generation. Journal of Thermal Engineering 2021;8:656–666. doi:https://doi.org/10.18186/thermal.1190558.

[28] Al-Sanea S, Mujahid A. A numerical study of the thermal performance of fins with time-dependent boundary conditions, including initial transient effects. W¨arme-und Stoff¨ubertragung 1993;28:417–424. doi:10.1007/BF01577883.

[29] Sobamowo GM, Ogunmola BY, Nzebuka G. Finite volume method for analysis of convective longitudinal fin with temperature-dependent thermal conductivity and internal heat generation. in: Defect and Diffusion Forum, 2017;374:106–120. doi:10.4028/www.scientific.net/DDF.374.106.

[30] Khani F, Raji MA, Nejad HH. Analytical solutions and efficiency of the nonlinear fin problem with temperature-dependent thermal conductivity and heat transfer coefficient. Communications in Nonlinear Science and Numerical Simulation 2009;14:3327–3338. doi:10.1016/j.cnsns.2009.01.012

[31] Vyas PD, Thakur HC, Darji VP. Nonlinear analysis of convective-radiative longitudinal fin of various profiles. International Journal of Numerical Methods for Heat & Fluid Flow 2020;30:3065–3082. doi:10.1108/HFF-08-2018-0444.

[32] Bergman TL, Lavine AS, Incropera FP, DeWitt DP. Introduction to heat transfer. John Wiley & Sons, Hoboken, NJ; 2011.